



Published in final edited form as:

J Biomed Mater Res A. 2014 July ; 102(7): 2173–2180. doi:10.1002/jbm.a.34902.

Immunotherapy with Injectable Hydrogels to Treat Obstructive Nephropathy

Danielle E. Soranno¹, Hoang D. Lu², Heather M. Weber², Reena Rai², and Jason A. Burdick^{2,*}

¹Children's Hospital of Philadelphia, University of Pennsylvania, Philadelphia, PA

²Department of Bioengineering, University of Pennsylvania, Philadelphia, PA

Abstract

Hydrogels are gaining attention as injectable vehicles for delivery of therapeutics for a range of applications. We describe self-assembling and injectable Dock-and-Lock hydrogels for local delivery of interleukin-10 (IL-10) to abate the progression of inflammation and fibrosis that leads to chronic kidney disease. As monitored with a fluorescent tag, hydrogels degraded within a few days *in vitro* and matched IL-10 release profiles; however, hydrogels remained in the kidney for up to 30 days *in vivo*. A unilateral ureteral obstruction (UUO) mouse model was used to investigate *in vivo* outcomes after hydrogel injection and IL-10 delivery. Eight groups were investigated (7, 21, 35 days, n=4): healthy, sham, healthy injected with mouse serum albumin (MSA), healthy + hydrogel, UUO, UUO + IL-10, UUO + hydrogel, UUO + hydrogel/IL-10. 15 μ L of IL-10, hydrogel, or hydrogel/IL-10 was injected under the renal capsule 3 days after the UUO. Immunohistochemistry (IHC) was performed on paraffin sections to identify macrophages and apoptotic cells and trichrome staining was used to evaluate fibrosis. There were no significant differences in inflammatory markers between all control groups. With hydrogel delivery, macrophage infiltration and apoptosis were significantly reduced at days 21 and 35 compared to untreated animals. By day 35, IL-10 delivery via hydrogel reduced macrophage infiltration and apoptosis more than IL-10 injection alone. Fibrosis was decreased by day 35 in all treatment groups. This work supports the use of hydrogel delivery of IL-10 to treat chronic kidney disease.

Keywords

hydrogel; nephropathy; kidney; inflammation; drug delivery

INTRODUCTION

Congenital obstructive nephropathy is the leading cause of chronic kidney disease (CKD) in children. Despite early surgical repair, upwards of 50% of affected children go on to develop end-stage renal disease (ESRD), requiring renal replacement therapy in the form of either hemodialysis, peritoneal dialysis, or renal transplant¹. Children with CKD who progress to ESRD also have vastly decreased life expectancy secondary to metabolic bone disease and

*Corresponding author: Jason A. Burdick, Ph.D, 240 Skirkanich Hall, Philadelphia PA 19104, P: 215.898.8537, F: 215.573.2071, Burdick2@seas.upenn.edu.

poor cardiovascular outcomes². The cellular mechanisms of kidney injury caused by obstructive uropathy are multifactorial, including interstitial inflammation, interstitial fibrosis, and apoptosis³. In response to obstruction, macrophages release tumor necrosis factor- α (TNF α) and transforming growth factor- β 1 (TGF β 1) which induce more interstitial fibrosis and apoptosis with consequential ischemic injury and kidney damage^{4,5}. Interleukin-10 (IL-10) is a target molecule for delivery for its potent anti-inflammatory properties, with inhibition of cytokine production and mononuclear cell function^{6,7}.

Hydrogels are water-swollen polymer networks that can be created with a broad range of mechanical and structural properties, as well as the ability to be injected directly into tissues. They can be engineered to deliver an array of therapeutics, including cytokines, drugs, or stem cells. By varying their chemical properties, hydrogels can be formulated with varying crosslink density, association between the hydrogel and entrapped molecules, and degradation rates. These properties influence the rate of molecule delivery from hydrogels and can be engineered for release from hours to months. Importantly, the delivery of molecules locally to targeted tissues has the benefit of optimizing local efficacy while minimizing systemic side effects. To date, studies have evaluated the inflammatory response to injection of polymer biomaterials into the kidney, as well as the use of hydrogels to deliver therapeutics locally to the kidney or to aid in nephrological surgical procedures⁸⁻¹³.

The overall goal of this study was to test injectable hydrogels as a therapeutic option for obstructive nephropathy. Surgically created urinary tract obstruction in animal models can be manipulated with respect to severity and duration of obstruction to induce renal injury^{5,14}. Rodent models can be used to simulate and study the pathogenesis of obstructive nephropathy in the human kidney. Specifically, we used a unilateral ureteral obstruction in a wild-type mouse to induce obstructive uropathy in one kidney while leaving the contralateral kidney unaffected, with histological assessment of macrophage infiltration, apoptosis and fibrosis used to assess therapies. One of the benefits of the UUO model is that the contralateral kidney remains functional, so the animal remains healthy throughout the experiment. However, this also means that serum measurements of blood urea nitrogen and creatinine remain normal, and cannot be used to assess the utility of therapeutic intervention.

Although there are many hydrogels that are potentially useful for the delivery of IL-10 in this model, we recently developed self-assembling Dock-and-Lock (DnL) hydrogels that possess shear-thinning and self-healing properties that are particularly useful for this application¹⁵. The ability of the DnL hydrogels to shear-thin allows them to be injected into tissue via a syringe, and the rapid self-healing permits localization of the hydrogel and cargo at the injection site. Additionally, the hydrogel dissociation properties can be manipulated to allow for fast or slow erosion, which controls the release profiles of encapsulated cytokines. As reported previously¹⁵, this specific system was engineered to utilize the docking and dimerization domain (DDD) of cAMP-dependent protein kinase A with the anchoring domain (AD) of A-kinase anchoring proteins. The AD was conjugated to the ends of a four arm polyethylene glycol (PEG) (4aPEG-AD) (Figure 1) to permit formation of a hydrogel using biological derived interactions.

MATERIALS AND METHODS

Hydrogel formulation and characterization

Injectable Dock-n-Lock gels were developed as previously reported¹⁵ (Figure 1) and utilize the docking and dimerization domain (DDD) of c-AMP-dependent protein kinase A with the anchoring domain (AD) of A-kinase anchoring proteins. The AD was conjugated to the ends of four-arm polyethylene glycol (4aPEG), whereas the DDD was engineered into a telechelic polypeptide, and Cy 5.5 was conjugated to the primary amines of the AD peptide. One hydrogel system was used in this study that consisted of 3 wt% of rDDD and 2 wt% of 4aPEG AD. IL-10 was added to the gel or phosphate buffered saline solution at a concentration of 0.33 $\mu\text{g}/\mu\text{L}$ resulting in 5 μg of IL-10 delivered per 15 μL injection. *In vitro* gel erosion studies were performed on the 4aPEG-AD as previously described¹⁵ with samples incubated at 37° C and 4APEG-AD release measured by excitation/emission at 673/707 nm of the Cy 5.5 conjugate. ELISA (eBioscience) was used to quantify the amount of IL-10 in each sample to measure release as a function of hydrogel erosion.

Study design and animals

BALB/c mice were procured (JAX) for the animal study. Eight cohorts were studied (7, 21, 35 days, n=4): healthy, sham operation, healthy injected with MSA, healthy injected with hydrogel, unilateral ureteral obstruction (UUO), UUO injected with IL-10, UUO injected with hydrogel, UUO injected with hydrogel and IL-10. 15 μL of IL-10, hydrogel, or hydrogel with IL-10 was injected into the left kidney via retroperitoneal approach 3 days after the initial ureteral obstruction or sham operation. The hydrogel was injected into healthy kidneys to assess overall biocompatibility and to assess for inflammation due to the hydrogel alone. Healthy kidneys were injected with MSA suspended in PBS to assess for inflammation due to the injection. The sham cohort accounted for inflammation secondary to the surgical manipulation of the kidney. The treatment groups compared delivery of IL-10 alone, hydrogel alone, and hydrogel with IL-10. The dose of IL-10 delivered was 5 $\mu\text{g}/$ injection. The study was approved by the University of Pennsylvania's Institutional Animal Care and Use Committee, and adhered to the NIH Guide for the Care and Use of Laboratory Animals.

In vivo optical imaging of hydrogel degradation

Mice were placed on a special diet of TestDiet AIN 76A to minimize signal noise of Cy 5.5. The fluorescent marker Cy 5.5 was covalently bonded to the AD-peptide to allow for *in vivo* optical imaging and quantification of gel degradation (LICOR), in photons/pixel/second. The MSA was also labeled with Cy 5.5 to compare the dispersion of unencapsulated protein (MSA in phosphate buffered saline) to the degradation and clearance of the hydrogel. Animals were imaged daily for 5 days, then every other day until study time-points were reached. Intensities were normalized for each mouse and then averaged per cohort. An exponential decay model was applied to determine the half-life of the injected MSA or hydrogel for each group.

Histological analysis

Kidneys were fixed in formalin and embedded in paraffin (4 μm thick). Immunohistochemistry (IHC) was performed to identify macrophages via rat anti-CD68 IgG (1:100) (abcam) and biotinylated goat anti-rat IgG (1:200) (abcam). Specimens were incubated with the primary antibody overnight at 4°C. Blocking agents included 20% goat serum (Vector Laboratories) and Avidin and Biotin block (Vector Laboratories). Terminal deoxynucleotidyl transferase dUTP nick end labeling (TUNEL) assay was used to assess for apoptotic cells (Invitrogen). Vectastain ABC kit (Vector Laboratories) was used for immunoperoxidase staining, and specimens were counterstained with hematoxylin. Trichrome stain (American MasterTech) was used to evaluate fibrosis. Cells and total area were quantified (20 images/section) at 400 \times magnification for IHC and TUNEL, and total fibrotic area was quantified for trichrome using computer software (Image J). Cohorts were blinded until quantitative histological analysis was complete. ANOVA with Tukey post-hoc analysis was used to determine statistical significance amongst the control and treatment groups.

RESULTS

Hydrogel formation and IL-10 release

DnL hydrogels were fabricated as reported previously¹⁵ and one formulation was used in this study that consisted of 2wt% 4aPEG-AD and 3wt% rDDD, permitting rapid hydrogel assembly when the two components were mixed (Figure 1). After hydrogel encapsulation, IL-10 release (measured via ELISA) corresponded directly to hydrogel erosion (measured via rDDD absorption) (Figure 2). Within 48 hours of hydrogel incubation at 37° in PBS, ~70% of the hydrogel had eroded. Concordantly, ~87% of the total IL-10 released had been released by that time. Hydrogel erosion tapered towards complete dissolution around 80 hours, with a corollary cessation of IL-10 release. Thus, DnL hydrogels are useful for controlled molecule delivery.

In vivo monitoring of hydrogel erosion

Figure 3 shows serial images of the 4aPEG-AD DnL hydrogel after injection into healthy and obstructed kidneys as measured by the covalently bonded far-infrared marker Cy 5.5. MSA was also tagged with Cy 5.5 to compare the clearance of a protein injected into the kidney without a hydrogel carrier. Tagged DnL hydrogels both with and without IL-10 were injected into obstructed kidneys to assess for any influence of the IL-10 on hydrogel degradation. Figure 4 shows the fluorescence profiles after injection for either tagged hydrogels or MSA, as well as the time constants for loss of fluorescence. As seen in Figure 4A and 4C, MSA cleared faster than the 4aPEG-AD hydrogel when injected into healthy kidneys. The addition of IL-10 to the hydrogel did not affect degradation when injected into obstructed kidneys. The half-life for each group were: healthy injected with MSA 4.98 ± 0.3 days, healthy injected with hydrogel 6.38 ± 0.3 days, UUU injected with hydrogel 7.6 ± 1 days, UUU injected with hydrogel and IL-10 7.2 ± 1 days (Figure 4C). Unencapsulated molecules cleared faster than molecules delivered within the hydrogel carrier.

Hydrogel inflammatory response when injected into healthy kidneys

In the control groups (sham operation, healthy kidney injected with MSA, healthy kidney injected with hydrogel), there were no significant differences in macrophage infiltration (measured via CD68, Figure 5, 6A), apoptosis (measured via TUNEL assay, Figure 6B) or fibrosis (measured via trichrome, Figure 6C) after 7, 21 or 35 days when compared to healthy kidney. Specifically, healthy kidneys were injected with 15 μ L of 4aPEG-AD/rDD and compared to healthy kidneys, sham operated kidneys, and kidneys injected with 15 μ L of MSA in PBS and there were no statistical differences in these markers of inflammation. This indicates a general biocompatible response to material injection, and supports the use of 4aPEG-AD hydrogels as platform for biomolecule delivery into the kidney.

Macrophage infiltration in untreated and treated groups in the UUO model

The left column of Figure 5 shows a representative montage of IHC images of tissues stained for CD68 to assess macrophage infiltration 35 days after the UUO procedure. Healthy kidney and healthy kidney injected with hydrogel are shown for comparison to the untreated UUO model, and the UUO model treated with IL-10 alone, hydrogel alone and hydrogel with IL-10. Figure 7A shows the quantitative histological analysis of the immunohistochemistry for macrophage infiltration. In comparing the treatment groups (UUO injected with IL-10, UUO injected with hydrogel, UUO with hydrogel and IL-10) to the untreated UUO, there was a significant reduction in macrophage infiltration 21 days and 35 days after the initial UUO operation (18 days and 32 days status post injection of the IL-10, hydrogel, or hydrogel with IL-10). At 35 days, there was further statistical significance between the cohorts treated with IL-10 alone and hydrogel with IL-10, with less macrophage infiltration in the latter cohort. This suggests that controlled release of IL-10 over several weeks improves efficacy against macrophage infiltration compared to a bolus dose of IL-10 alone. Treatment with hydrogel alone also yielded an anti-inflammatory effect.

Apoptosis in untreated and treated groups in the UUO model

The center panel of Figure 5 shows representative images of tissue stained via TUNEL to assess for apoptosis 35 days post-obstruction. Healthy kidney and healthy kidney injected with hydrogel are shown for comparison to the untreated and treated UUO model. Figure 7B shows the quantitative analysis of the treatment groups compared to the untreated UUO. Apoptosis was significantly reduced in all three treatment groups at day 21, and only in the hydrogel alone and hydrogel with IL-10 at day 35. There was no significant reduction in the group treated with IL-10 alone at day 35 suggesting that delivery via hydrogel carrier and corresponding prolonged release is superior to bolus injection of IL-10 alone. As seen in the macrophage quantification, treatment with hydrogel alone showed beneficial anti-inflammatory effects in the injured model.

Fibrosis in untreated and treated groups in the UUO model

The right column of Figure 5 is a representative montage of the healthy and injured groups at the 35 day time-point stained via trichrome to assess for fibrosis. As seen in Figure 7C, all three treatment groups showed a significant decrease in percentage of fibrosis at the 35 day

time-point compared to the untreated UUO model. There was no statistical difference appreciated at the earlier time-points, nor was there any further difference seen amongst the treatment groups.

DISCUSSION

While much has been learned regarding pathogenesis and disease progression in chronic kidney disease, there has been a dearth of treatment options. Therapeutic options currently focus on delaying disease progression rather than therapies to correct or abate the disease process. Regardless of the underlying etiology of chronic kidney disease, there is a resultant pro-inflammatory milieu, which leads to inflammation, apoptosis and fibrosis. Once this process has begun, there is a resultant increase in local inflammation and loss of nephrons, leading to a vicious cycle of decreased functioning renal mass^{3,4}. Targeted drug delivery that could ameliorate these pro-inflammatory effects could decrease the amount of scarring and theoretically spare remaining renal function. Tunable and injectable biomaterials represent a novel therapeutic treatment option for renal disease, and there are a growing number of groups evaluating their use for either drug or cell delivery⁸⁻¹³. However, to our knowledge this study represents the first system of targeted drug delivery to treat obstructed kidneys via hydrogels.

Shear-thinning hydrogels were synthesized that permit facile local delivery of immunotherapy to both healthy and obstructed kidneys. Our study showed that DnL hydrogels are biocompatible and do not elicit a significant inflammatory response in the kidney when quantified via macrophage infiltration, apoptosis and fibrosis. Injecting the gel into healthy kidney did not induce inflammation or scarring, and all quantified markers were not statistically different than healthy or sham controls. Furthermore, delivery of the hydrogel alone had therapeutic anti-inflammatory effects when delivered to the injured model, with a significant decrease in macrophage infiltration and apoptosis at the 21 and 35 day time-points, and a decrease in fibrosis at the 35 day time-point. This surpassed the anti-inflammatory effect seen in the cohort treated with IL-10 alone. We hypothesize that the hydrogel may serve to quench the pro-inflammatory milieu, potentially via adsorption of cytokines with subsequent clearance as the gel degrades, or a direct effect on antigen presenting cells¹⁶. Serum markers of inflammation could further differentiate the efficacy of treatment with hydrogel, IL-10 or both hydrogel/IL-10, and we plan to include these markers in future studies.

DnL gels are clinically viable for further translational research as their delivery in human subjects would be similar to ultrasound-guided percutaneous renal biopsies. Our results show that the gel itself did not elicit a pro-inflammatory response nor result in tissue damage. By covalently bonding a far-IR marker to the injected hydrogels, we were able to follow gel degradation serially. Prior studies have relied on histological outcomes to gauge polymer erosion *in vivo* over time, or have simply mixed dyes with the polymer. The covalent attachment of the Cy 5.5 to the protein component of the hydrogel assured accurate tracking of the hydrogel as opposed to diffusion of a dye. The hydrogels used in our study had mostly degraded by three weeks after injection. As the injected kidney was completely obstructed, we hypothesize that local phagocytotic cells cleared the gel. Erosion properties

can be manipulated by changing the chemical configuration of the hydrogel components, which would allow for faster or slower gel degradation *in vivo* with corresponding delivery of encapsulated molecules¹⁵. We chose the specific hydrogel formulation for its relatively fast erosion time given the short half-life of IL-10, however, a longer erosion profile with more prolonged drug delivery can be engineered by changing the chemical structure of the gel. Similarly, a wide range of molecules at varying doses may be encapsulated within the hydrogel for sustained release over time.

In summary, renal inflammation and scarring was reduced in an animal model of chronic kidney disease by using an injectable hydrogel for delivery of IL-10. Our study showed a decrease in macrophage infiltration, apoptosis and fibrosis in an animal model of obstructive uropathy treated with IL-10 via an injectable hydrogel. Delivery of IL-10 via hydrogel versus an injection of IL-10 alone, allowed for prolonged drug release and showed therapeutic benefits, particularly with regard to macrophage infiltration and apoptosis 5 weeks status post obstruction. Current treatment options for CKD are limited, and injectable hydrogels are a novel and clinically viable option to deliver therapeutics to abate disease progression. While early surgical repair remains essential, concordant surgical repair and medical treatment via targeted drug delivery could have synergistic benefits to patients with obstructive nephropathy. Importantly, the development of a delivery system that targets inflammatory mediated kidney injury could have further implications in the treatment of a multitude of kidney diseases, both acute and chronic. Both cell therapy and anti-inflammatory molecules could be delivered to target the pro-inflammatory cycle that results in renal scarring and insufficiency^{4,6,17–22}. Further studies are warranted, and inclusion of serum markers of inflammation would help to characterize any anti-inflammatory properties of the hydrogel itself.

Acknowledgments

We thank David Wasserman, Ph.D for his expertise with the use of the LI-COR Pearl for optical imaging. We are grateful for support from the National Institute of Health and Dr. Lawrence Holzman M.D. at the University of Pennsylvania for a clinical fellow's training grant (DES), the Institute of Regenerative Medicine at the University of Pennsylvania for a Pilot Study Grant, and Graduate Research Fellowship (HDL) from the National Science Foundation.

REFERENCES

1. Roth K, Carter W, Chan J. Obstructive nephropathy in children: long-term progression after relief of posterior urethral valve. *Pediatrics*. 2001; 107:1004–1010. [PubMed: 11331678]
2. Groothoff J. Long-term outcomes of children with end-stage renal disease. *Pediatr Nephrol*. 2005; 20:849–853. [PubMed: 15834618]
3. Chevalier R, Thornhill B, Forbes M, Kiley SC. Mechanisms of renal injury and progression of renal disease in congenital obstructive nephropathy. *Pediatr Nephrol*. 2010; 25:687–697. [PubMed: 19844747]
4. Klahr S, Morrissey JJ. The role of vasoactive compounds, growth factors and cytokines in the progression of renal disease. *Kidney Int*. 2000; 57:S7–S14.
5. Lange-Sperandio B, Fulda S, Vandewalle A, Chevalier RL. Macrophages induce apoptosis in proximal tubule cells. *Pediatr Nephrol*. 2003; 18:335–341. [PubMed: 12700958]
6. Tayal V, Kalra B. Cytokines and anti-cytokines as therapeutics – An update. *Eur J of Pharmacology*. 2008; 579:1–12.

7. Dhande I, Ali Q, Hussain T. Proximal Tubule Angiotensin AT2 Receptors Mediate an Anti-Inflammatory Response via Interleukin-10: Role in Renoprotection in Obese Rats. Hypertension. 2013 , in press.
8. Dankers P, van Luyn M, Huizinga-van der Vlag A, van Gemert GML, Petersen AH, Meijer EW, Janssen HM, Bosman AW, Popa ER. Development and in-vivo characterization of supramolecular hydrogels for intrarenal drug delivery. *Biomaterials*. 2012; 33:5144–5155. [PubMed: 22494885]
9. Basu J, Genheimer C, Rivera E, Payne R, Mihalko K, Guthrie K, Bruce AT, Robbins N, McCoy D, Sangha N, Ilagan R, Knight T, Spencer T, Wagner BJ, Jayo MJ, Jain D, Ludlow JW, Halberstadt C. Functional Evaluation of Primary Renal Cell/Biomaterial Neo-Kidney Augment Prototypes for Renal Tissue Engineering. *Cell Trans*. 2011; 20:1771–1790.
10. Gao J, Liu R, Wu J, Liu ZQ, Li JJ, Zhou J, Hao T, Wang Y, Du ZY, Duan CM, Wang CY. The use of chitosan based hydrogel for enhancing the therapeutic benefits of adipose-derived MSCs for acute kidney injury. *Biomaterials*. 2012; 33:3673–3681. [PubMed: 22361096]
11. Gheisari Y, Yokoo T, Matsumoto K, Fukui A, Sugimoto N, Ohashi T, Kawamura T, Hosoya T, Kobayashi E. A thermoreversible polymer mediates controlled release of glial cell linederived neurotrophic factor to enhance kidney regeneration. *Artif Organs*. 2010; 34:642–647. [PubMed: 20497162]
12. Ramakumar S, Phull H, Purves T, Funk J, Copeland D, Ulreich JB, Lai LW, Lien YHH. Novel Delivery of oligonucleotides using a topical hydrogel tissue sealant in a murine partial nephrectomy model. *J Urol*. 2005; 174:133–136.
13. Bernie JE, Ng J, Bargman V, Gardner T, Cheng L, Sundaram CP. Evaluation of hydrogel tissue sealant in porcine laparoscopic partial-nephrectomy model. *J Endourol*. 2005; 19:1122–1126. [PubMed: 16283851]
14. Chevelier R, Forbes M, Thornhill B. Ureteral obstruction as a model of renal interstitial fibrosis and obstructive nephropathy. *Kidney Int*. 2009; 75:1145–1152. [PubMed: 19340094]
15. Lu H, Charati M, Kim I, Burdick JA. Injectable Shear-Thinning Hydrogels Engineered with a Self-Assembling Dock-and-Lock Mechanism. *Biomaterials*. 2012; 33:2145–2153. [PubMed: 22177842]
16. Hubbell J, Thomas S, Swartz M. Materials Engineering for immunomodulation. *Nature*. 2009; 462:449–460. [PubMed: 19940915]
17. Lin C, Metters A, Anseth K. Functional PEG-peptide hydrogels to modulate local inflammation induced by the pro-inflammatory cytokine TNF α . *Biomaterials*. 2009; 30:4907–4914. [PubMed: 19560813]
18. Miyajima A, Chen J, Lawrence C, Ledbetter S, Soslow RA, Stern J, Jha S, Pigato J, Lemer ML, Poppas DP, Vaughan ED, Felsen D. Antibody to transforming growth factor- β ameliorates tubular apoptosis in unilateral ureteral obstruction. *Kidney Int*. 2000; 58:2301–2313. [PubMed: 11115064]
19. Misseri R, Meldrum DR, Dinarello CA, Dagher P, Hile KL, Rink RC, Meldrum KK. TNF α mediates obstruction-induced renal tubular cell apoptosis and proapoptotic signaling. *Am J Physiol Renal Physiol*. 2005; 288:F406–F411. [PubMed: 15507546]
20. Imai N, Kaur T, Rosenberg M, Gupta S. Cellular therapy of kidney diseases. *Semin Dial*. 2009; 22:629–635. [PubMed: 20017833]
21. Bussolati B, Hauser P, Carvalhosa R, Camussi G. Contribution of stem cells to kidney repair. *Curr Stem Cell Res Ther*. 2009; 4:2–8. [PubMed: 19149624]
22. Asanuma H, Meldrum D, Meldrum K. Therapeutic applications of mesenchymal stem cells to repair kidney injury. *J Urol*. 2010; 184:26–33. [PubMed: 20478602]

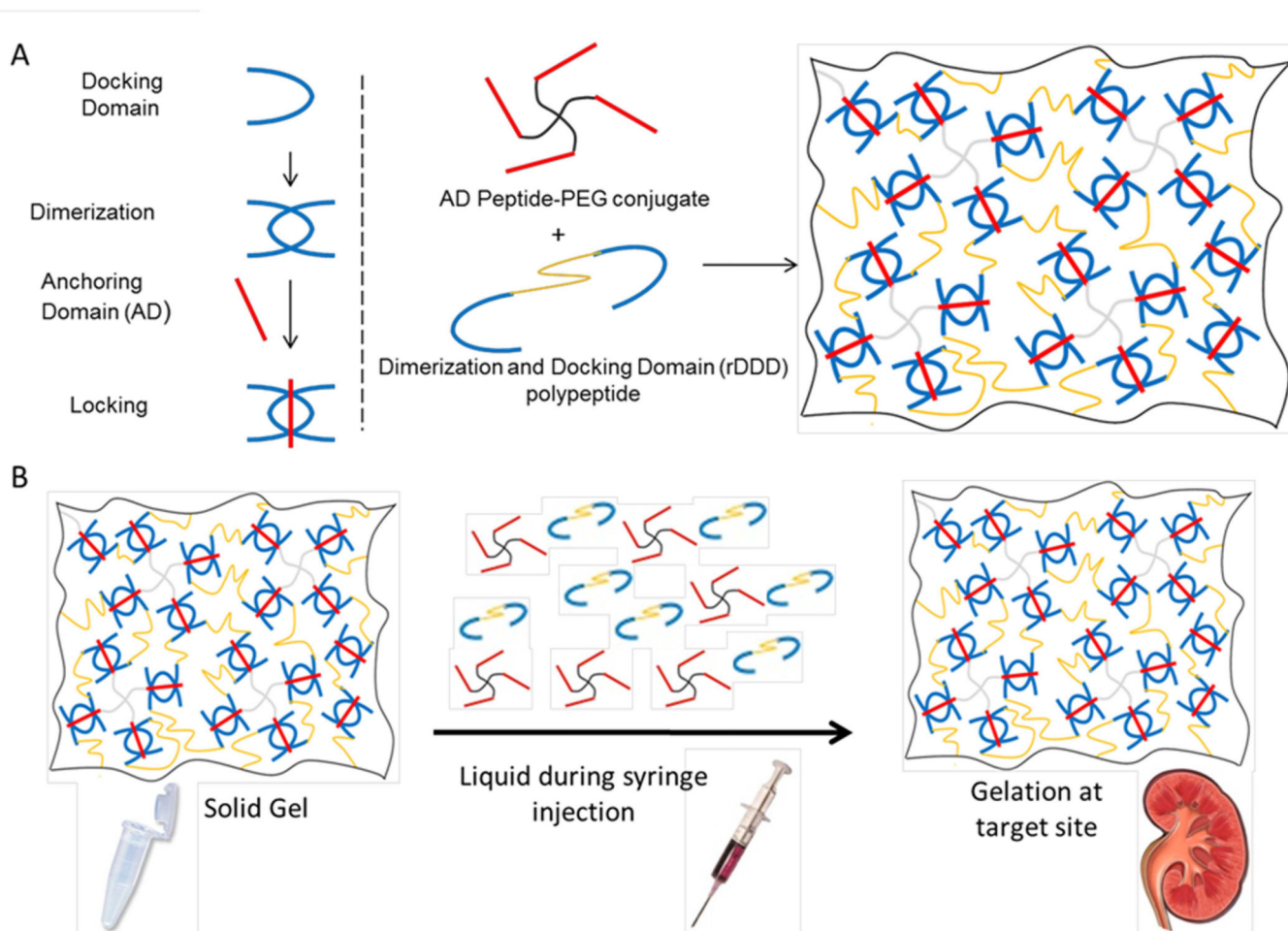


Figure 1.

(A) Schematic of the Dock-and-Lock (DnL) hydrogel system. The dimerization and docking domain polypeptides (rDDD) assemble through dimerization into long chains (“dock”) that are then crosslinked through interactions of the dimers with the anchoring domains (AD) attached to multi-arm poly(ethylene glycol) (“lock”) to form hydrogels. (B) The shear-thinning properties (disassembly with application of shear, rapid reassembly with shear removal) of the DnL hydrogels permits subcapsular renal injection.

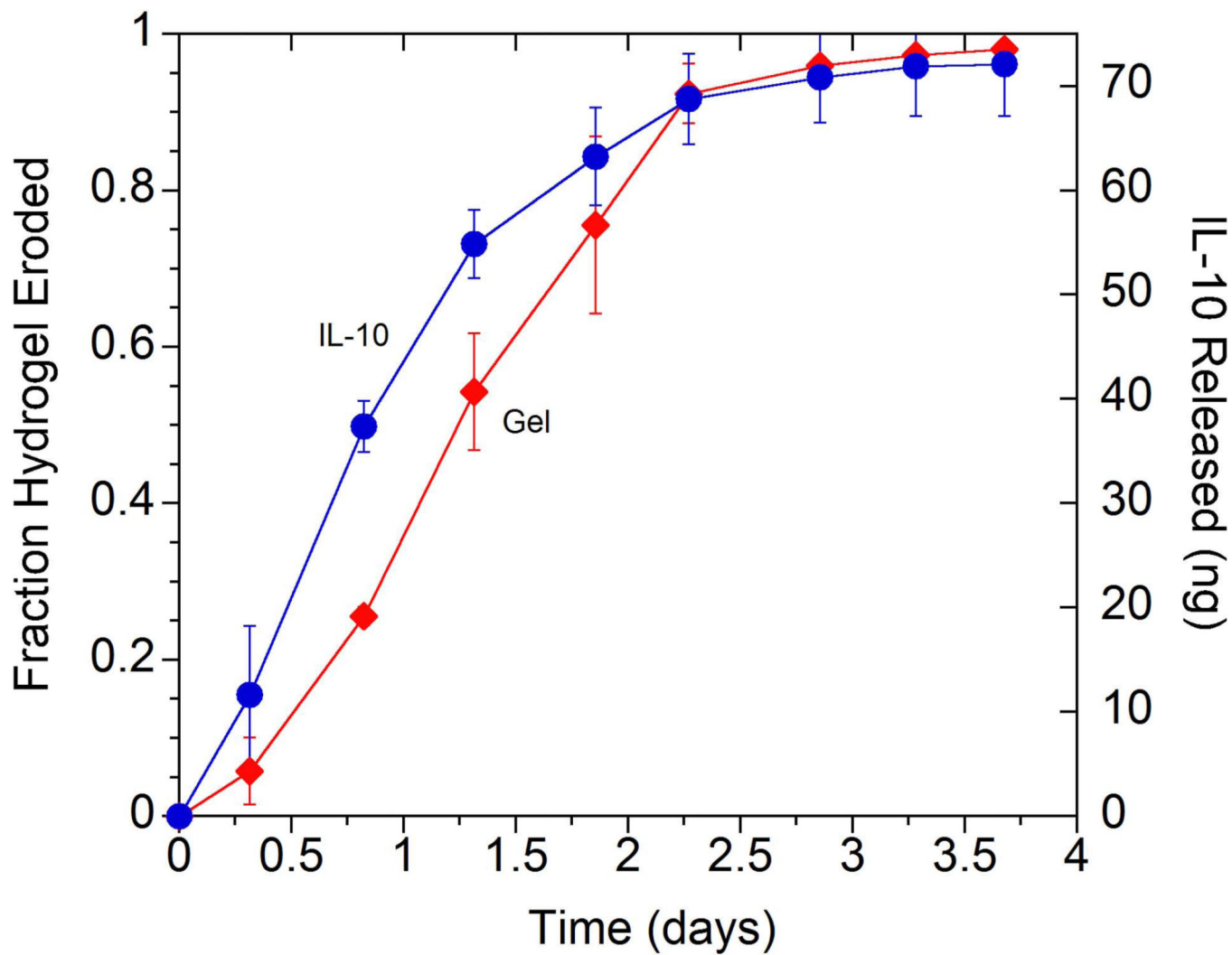


Figure 2.
In vitro DnL hydrogel erosion and corresponding release of IL-10 over time. The DnL hydrogels are formed through dynamic bonds that disassemble with time and release IL-10 to the environment.

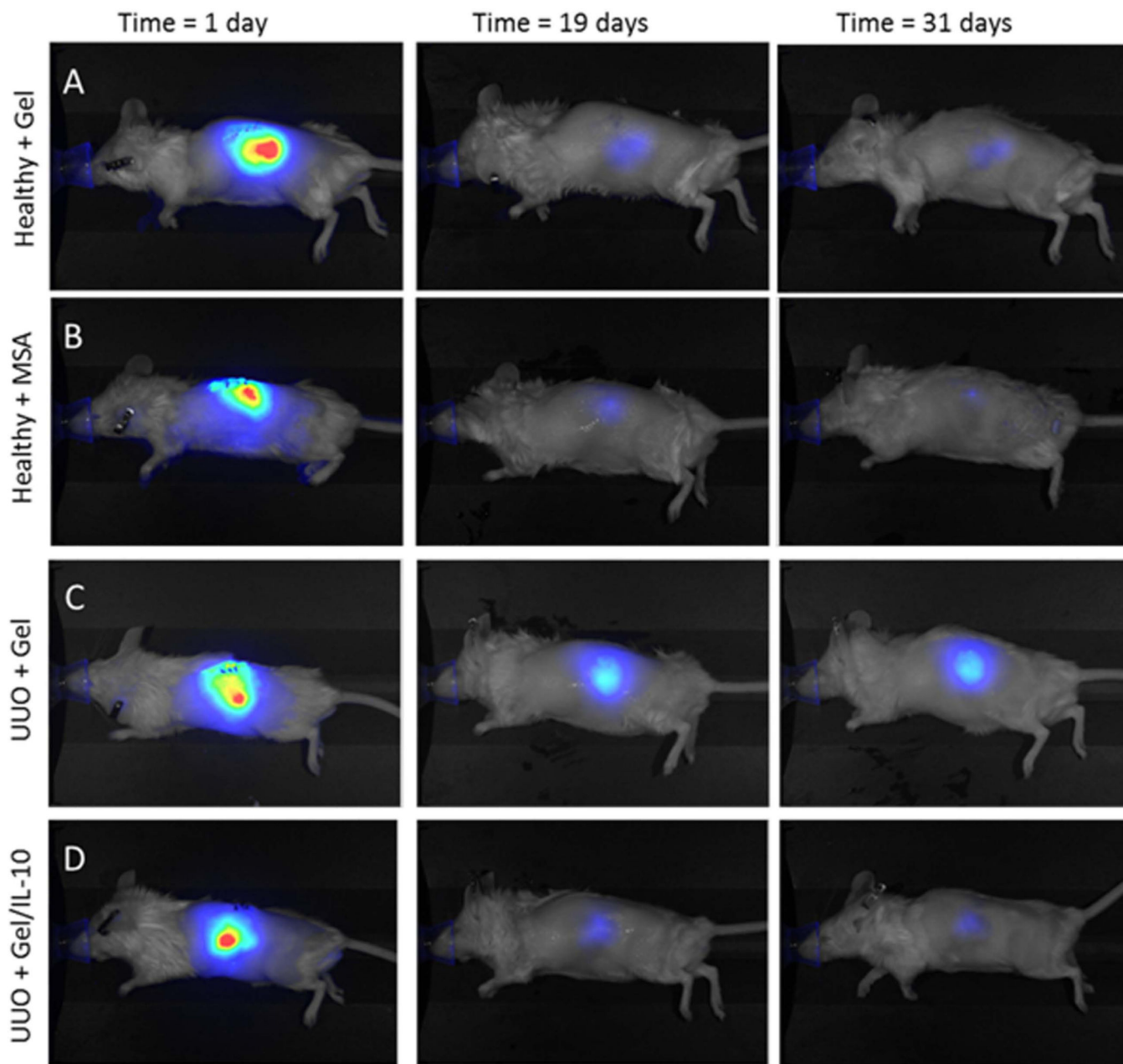


Figure 3. Serial *in vivo* optical images of the far IR-marker Cy 5.5 covalently bonded to either the AD peptide in the DnL hydrogels (**A**) or directly to MSA (**B**). When injected into healthy kidneys, the MSA diffused and cleared at a faster rate than the DnL hydrogel. Labeled DnL hydrogels were also injected into obstructed kidneys either without (**C**) or with IL-10 (**D**), illustrating that the addition of IL-10 did not affect degradation.

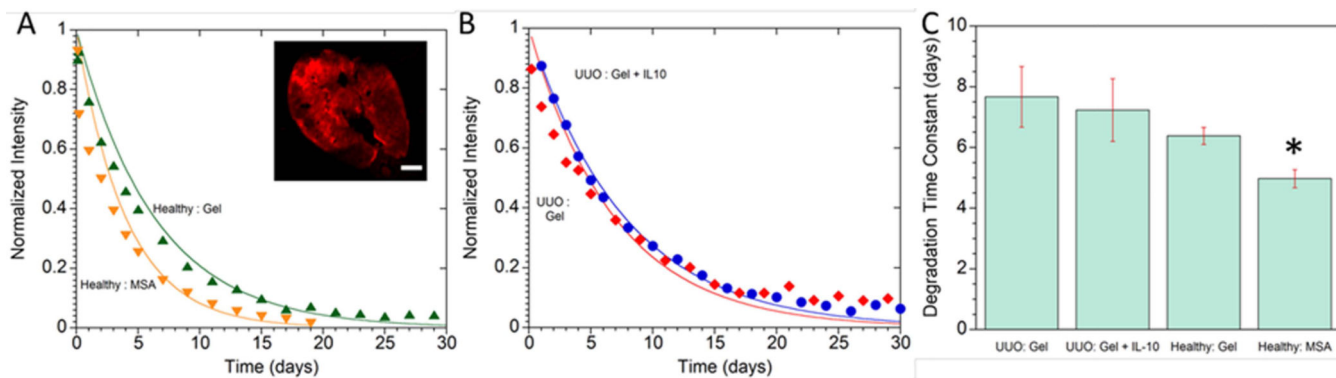


Figure 4.

Quantification of Cy 5.5 signal after injection of labeled hydrogels or MSA into kidneys. **(A)** MSA cleared faster than the DnL hydrogel when injected into healthy kidneys. Inset: Cross section of healthy kidney after injection with Cy 5.5-labeled DnL hydrogel, scale bar = 500 μm . **(B)** Hydrogels with and without IL-10 exhibited similar erosion rates when injected into obstructed kidneys. **(C)** Degradation time constants for hydrogel erosion or MSA clearance after injection into either obstructed or healthy kidney. *denotes statistical significance ($p < 0.05$) when compared to all other groups.

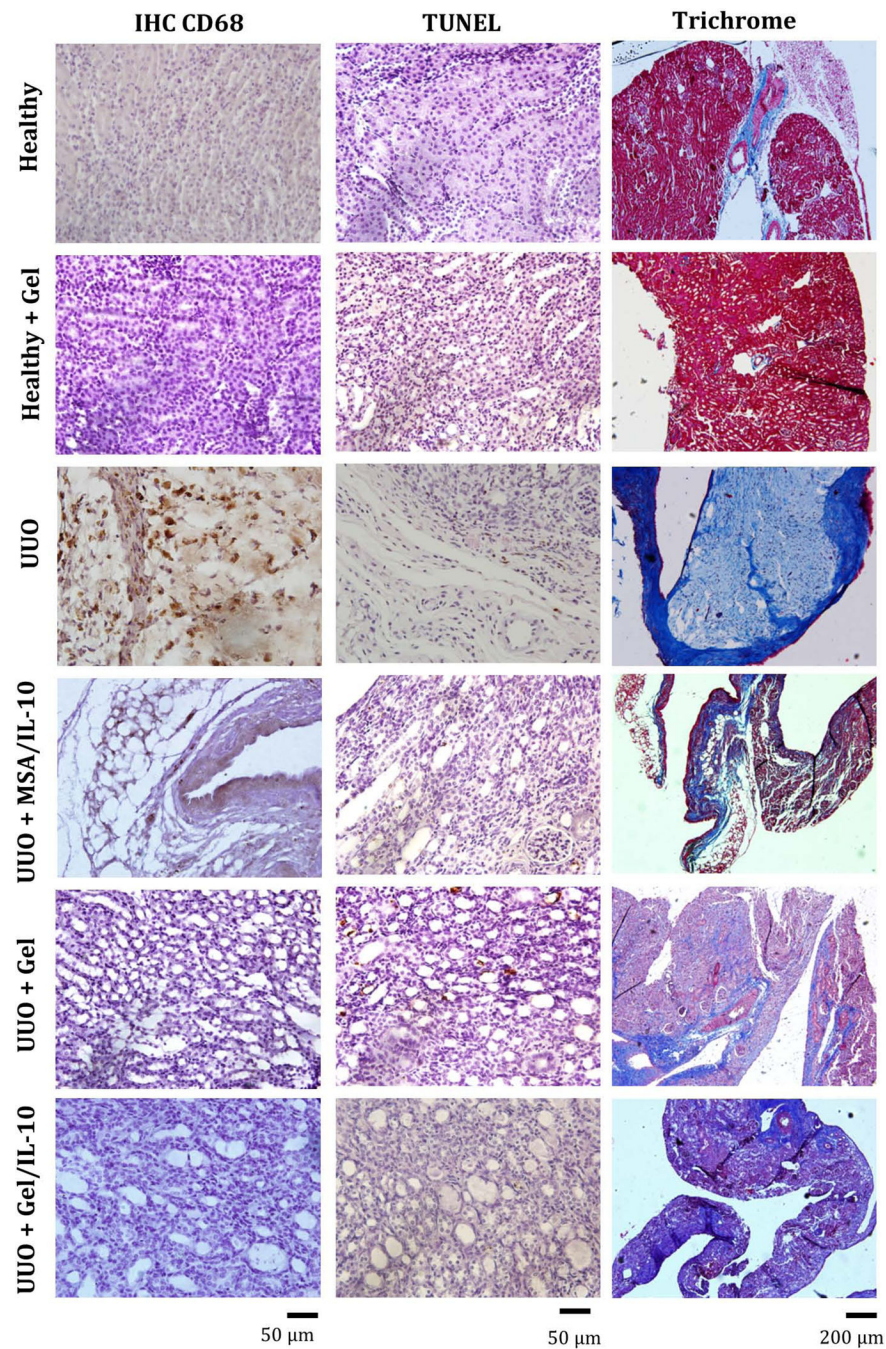


Figure 5. Histology Montage of Day 35 Time-point. Left column: Montage of IHC for CD68 to assess macrophage infiltration. Center column: TUNEL stain to assess apoptotic cells. For both IHC CD68 and TUNEL analysis, twenty digital images were captured at 400 \times magnification for each tissue sample, n=4 at time-points 7, 21 and 35 status-post obstruction or sham. Positive cells were averaged per group and ANOVA with Tukey post-hoc was used to determine statistical significance. Right column: Montage of Trichrome stains to assess for fibrosis. Digital images were captured at 40 \times magnification for the entire area of each tissue

sample, n=4 at time-points 7, 21 and 35 days status-post obstruction or sham. Imaging analysis quantified the percent of fibrotic area.

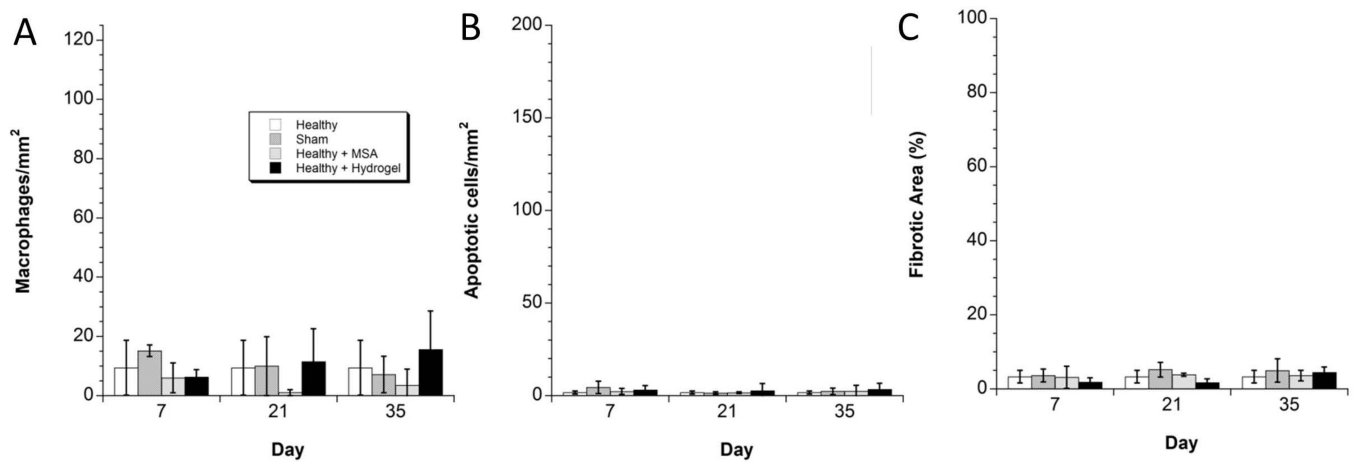


Figure 6.

Quantitative Analysis of the Control Groups. (A) In the control groups, there were no statistically significant differences in macrophages/mm² at any time-point. Injecting the hydrogel into healthy kidney did not incite macrophage infiltration. (B) In the control groups, there were no statistically significant differences in apoptotic cells/mm² at any time-point. Injecting the hydrogel into healthy kidney did not incite apoptosis. (C) In the control groups, there were no statistically significant differences in percentage of fibrosis at any time-point. Injecting the hydrogel into healthy kidney did not incite fibrosis.

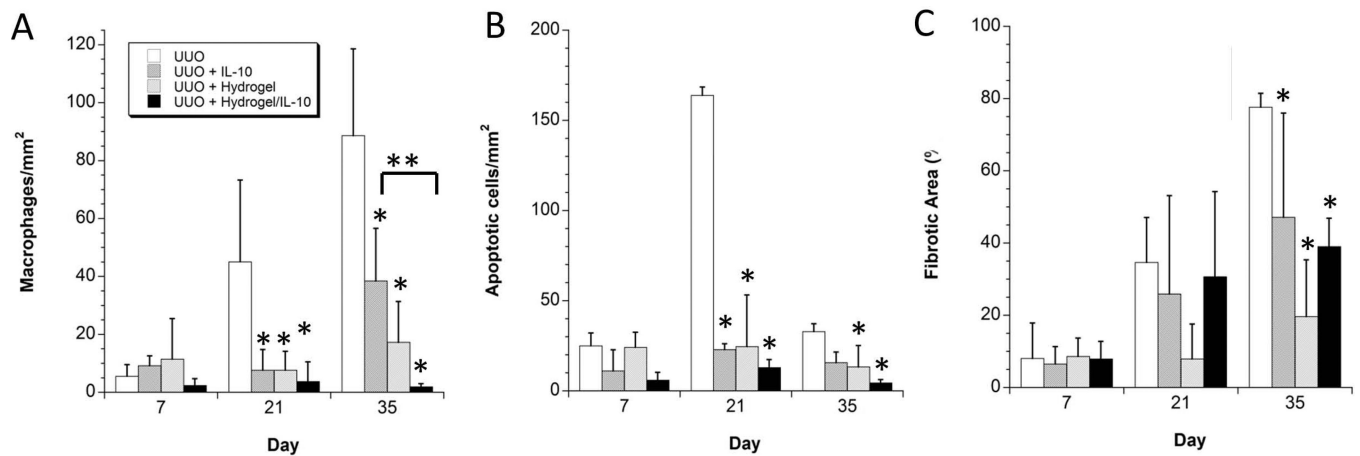


Figure 7.

Quantitative Analysis of the Treatment Groups. (A) Amongst the treatment groups, there was statistical significance in the reduction of macrophage infiltration at 21 and 35 days compared to the untreated UVO model. Injecting hydrogel + IL-10 showed further significance than IL-10 alone at the 5 week time-point. (B) Amongst the treatment groups, there was a significant reduction of apoptosis in all treatment groups 3 weeks post-obstruction, while at 5 weeks only the hydrogel and hydrogel + IL-10 showed a significant decrease in apoptosis. (C) Amongst the treatment groups, there was a significant reduction of fibrosis in all treatment groups 5 weeks post-obstruction.

*denotes statistical significance ($p < 0.05$) when compared to the control UVO group at that time point. **denotes statistical significance ($p < 0.05$) between marked groups.